Multiphase MCM/CAPRAM modeling of formation and processing of secondary aerosol constituents observed at the Mt. Tai summer campaign 2014

Yanhong Zhu [1, 2, a], Andreas Tilgner [2], Erik Hans Hoffmann [2], Hartmut Herrmann [2, 3 *], Kimitaka Kawamura [4, b], Lingxiao Yang [1], Likun Xue [1 *], Wenxing Wang [1]

[1] Environment Research Institute, Shandong University, 266237 Qingdao, China
[2] Leibniz Institute for Tropospheric Research (TROPOS), Atmospheric Chemistry Department (ACD), 04318 Leipzig, Germany
[3] School of Environmental Science and Engineering, Shandong University, 266237 Qingdao, China
[4] Institute of Low Temperature Science, Hokkaido University, Sapporo 060-0819, Japan
[a] Now at: Department of Atmospheric Sciences, School of Earth Sciences, Zhejiang University, 310012 Hangzhou, China
[b] Now at: Chubu Institute for Advanced Studies, Chubu University, Kasugai 487–8501, Japan

Correspondence to: Likun Xue (xuelikun@sdu.edu.cn), Hartmut Herrmann (herrmann@tropos.de)

Table S1. Emission data applied in the SPACCIM model.

Compound	Emission / molec cm^{-3} sec^{-1}	Compound	Emission / molec cm^{-3} sec^{-1}
Acetone	3.51E+04	Acetaldehyde	1.44E+04
Ethane	1.30E+05	Ethylene	1.76E+05
Propane	1.87E+05	Glyoxal	1.04E+04
n-Butane	6.79E+04	Formaldehyde	3.15E+04
Isobutane	2.99E+04	Biacetyl	1.49E+03
2,2-Dimethyl Butane	2.00E+03	Benzaldehyde	3.37E+02
Isopentane	6.75E+04	Isoprene	4.05E+05
n-Pentane	2.67E+04	Methacrolein	2.08E+03
2-Methyl Pentane	1.57E+04	Methyl ethyl ketone	8.68E+03
3-Methylpentane	1.10E+04	Methanol	2.28E+04
n-Hexane	6.28E+03	Methylglyoxal	3.93E+03
n-Heptane	4.71E+03	Methyl Vinyl Ketone	2.62E+02
2,3-Dimethyl Butane	4.71E+03	Propene	2.96E+04
n-Decane	1.77E+04	1-Hexene	2.45E+04
3-Methyl Hexane	1.77E+04	1-Butene	1.22E+04
n-Nonane	6.45E+03	1-Pentene	1.12E+04
n-Octane	6.45E+03	3-Methyl-1-Butene	3.06E+03
2-Methyl Hexane	4.84E+03	cis-2-Pentene	2.25E+04
n-Dodecane	3.22E+03	trans-2-Pentene	2.25E+04
n-Undecane	1.61E+03	1,3-Butadiene	9.64E+03
Toluene	1.39E+05	2-Methyl-2-Butene	8.03E+03
Ethyl Benzene	1.86E+04	Cis-2-Hexene	8.03E+03
n-Propyl Benzene	7.43E+03	Trans-2-Hexene	8.03E+03
Isopropyl Benzene	3.72E+03	Propionaldehyde	6.40E+03
m-Xylene	1.46E+04	a-pinene	2.99E+04
p-Xylene	1.46E+04	β-pinene	1.28E+04
o-Xylene	1.23E+04	Limonene	3.28E+02

1,2,3-Trimethyl Benzene	1.01E+04	Carbon monoxide	3.04E+07
1,3,5-Trimethyl Benzene	1.01E+04	Carbon dioxide	1.15E+09
m-Ethyl Toluene	5.61E+03	Ammonia	3.81E+06
o-Ethyl Toluene	5.61E+03	Nitric Oxide	2.51E+05
p-Ethyl Toluene	5.61E+03	Nitrogen dioxide	1.42E+06
1,2,4-Trimethyl Benzene	5.61E+03	Sulfur dioxide	1.91E+06

Table S2. Deposition velocities applied in the SPACCIM model.

Compound	**Deposition / s^{-1}**	**Compound**	**Deposition / s^{-1}**
Methanol	1.00E-05	N_2O_5	2.00E-05
Carbon monoxide	1.00E-06	Ammonia	1.00E-05
Ethanol	5.00E-06	Nitrogen dioxide	4.00E-06
Hydrogen peroxide	1.00E-05	Ozone	4.00E-06
Formaldehyde	1.00E-05	Formic acid	1.00E-05
Hydrochloric acid	1.00E-05	Sulfur dioxide	1.00E-05
Nitric acid	2.00E-05	Sulfuric acid	2.00E-05

Table S3. Initial gas-phase concentrations applied in the SPACCIM model.

Compound	**Concentration / molec cm^{-3}**	**Compound**	**Concentration / molec cm^{-3}**
Nitric oxide	7.76E+09	p-Xylene	2.28E+09
Nitrogen dioxide	4.14E+10	m-Xylene	2.28E+09
Ozone	2.42E+12	Acetaldehyde	2.42E+10
Nitric acid	1.62E+10	Propionaldehyde	1.70E+09
Hydrogen peroxide	7.57E+09	Butyraldehyde	8.52E+08
Formaldehyde	1.68E+10	Acetone	2.58E+10
Hydrogen	1.12E+13	Methyl ethyl ketone	7.10E+08
Carbon monoxide	2.84E+13	Methyl isobutyl ketone	3.14E+08
Methane	4.97E+13	Glyoxal	5.00E+09
Carbon dioxide	8.01E+15	Glycolaldehyde	5.00E+09

Sulfur dioxide	5.17E+10	Methylglyoxal	4.48E+08
Ethane	1.03E+10	Peroxyacetyl nitrate	2.24E+09
Propane	1.94E+09	Methyl hydrogen peroxide	4.48E+09
Isoprene	2.32E+09	Ethyl hydrogen peroxide	4.48E+08
n-propanol	3.14E+07	Peroxyacetic acid	4.48E+06
Isopropanol	1.23E+09	Ammonia	1.06E+11
Butanol	1.80E+07	Methanol	1.01E+10
Isobutanol	1.35E+07	Ethanol	9.56E+09
Ethylene glycol	2.82E+07	Glyoxylic acid	2.69E+09
Ethylene	2.32E+10	Glycolic acid	2.69E+09
Toluene	7.42E+09		
Cresol	4.48E+06		
o-Xylene	1.51E+09		

Table S4. Aerosol compositions and parameters applied in the SPACCIM model.

Compound	**Data / g/g**	**Parameter**	**Data**
Sulfate	0.25	Aerosol radius	2.0E-07 m
Nitrate	0.21	Aerosol water content	8.9E-08 l m^{-3}
Ammonium	0.16	Aerosol Density	1770 kg m^{-3}
Water-soluble organic carbon	0.07		
HULIS	0.07		
Water-insoluble organic carbon	0.05		
Positive monovalent ions	0.03		
Positive divalent ions	0.01		
Metals	0.03		
Elemental carbon	0.03		

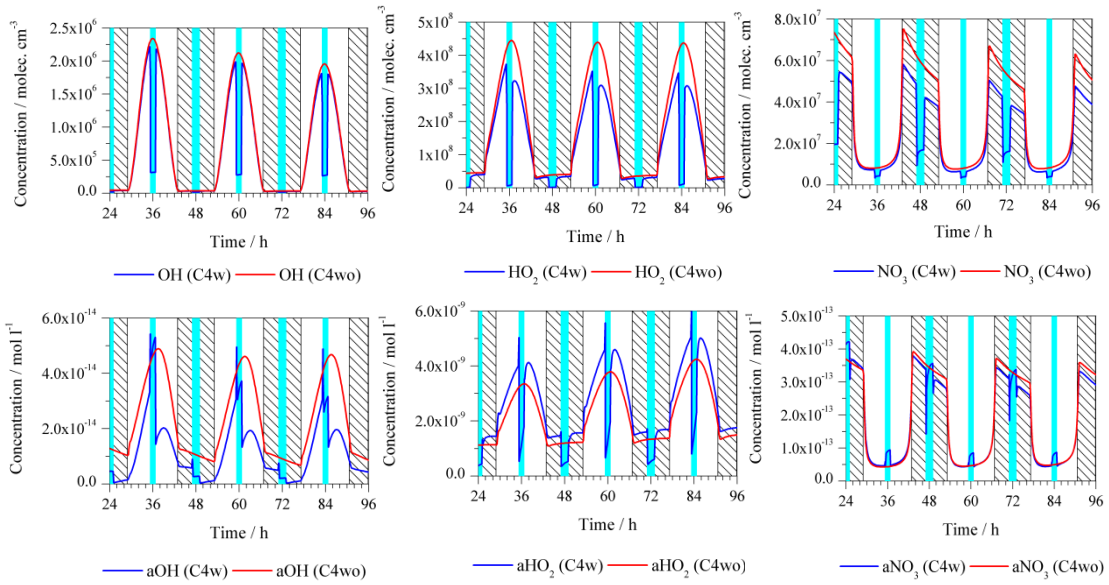

Figure S1. Time series of the modeled radical oxidant concentrations in the C4w and C4wo cases (light blue column: cloud; shadow: night).

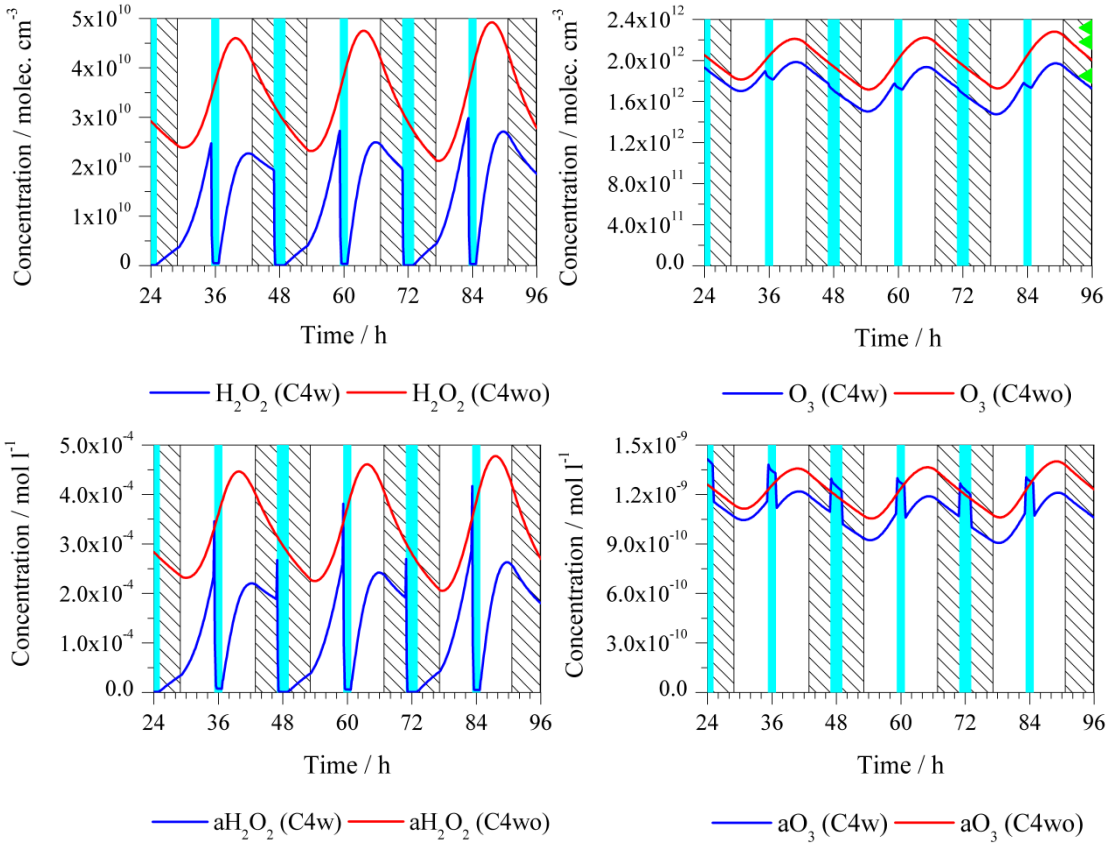

Figure S2. Time series of the modeled non-radical oxidant concentrations in the C4w and C4wo cases (light blue column: cloud; shadow: night; green triangle: maximum (above), average (middle) and minimum (below) value of measured concentration at Mt. Tai).

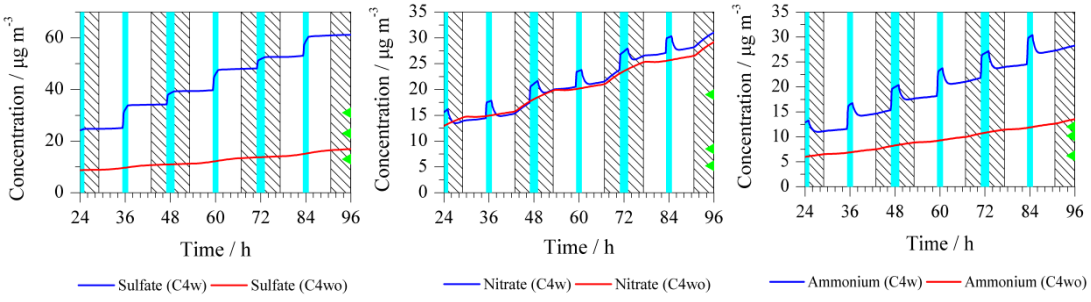

Figure S3. Time series of the modeled concentrations of key secondary inorganic ions in the C4w and C4wo cases (light blue column: cloud; shadow: night; green triangle: maximum (above), average (middle) and minimum (below) value of measured concentrations at Mt. Tai).

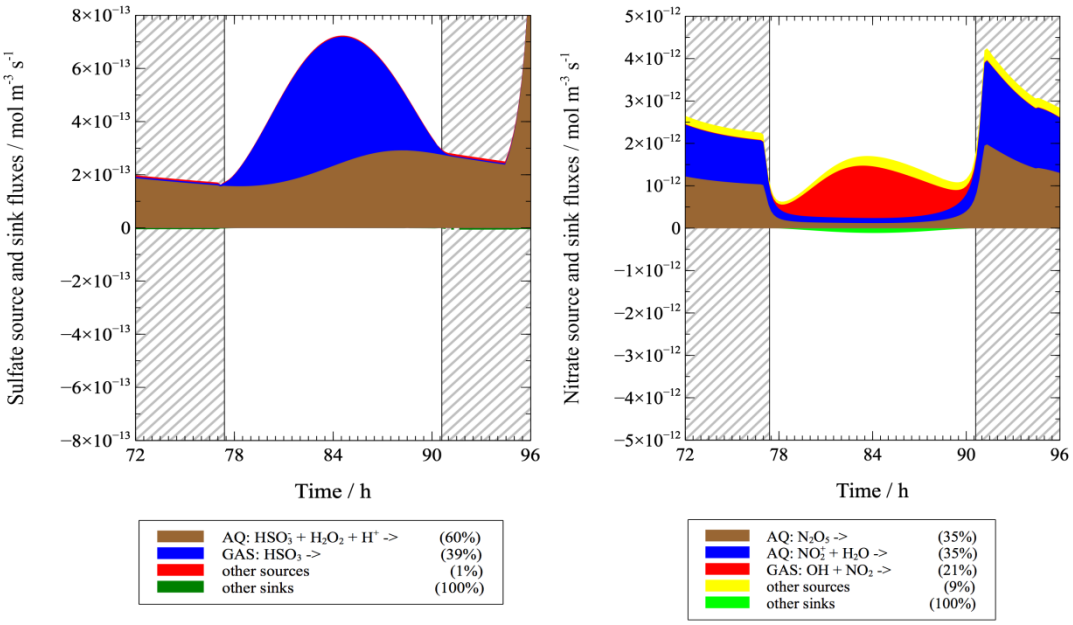

Figure S4. Modeled source and sink fluxes of sulfate (left) and nitrate (right) in the C2wo case (shadow: night).

75

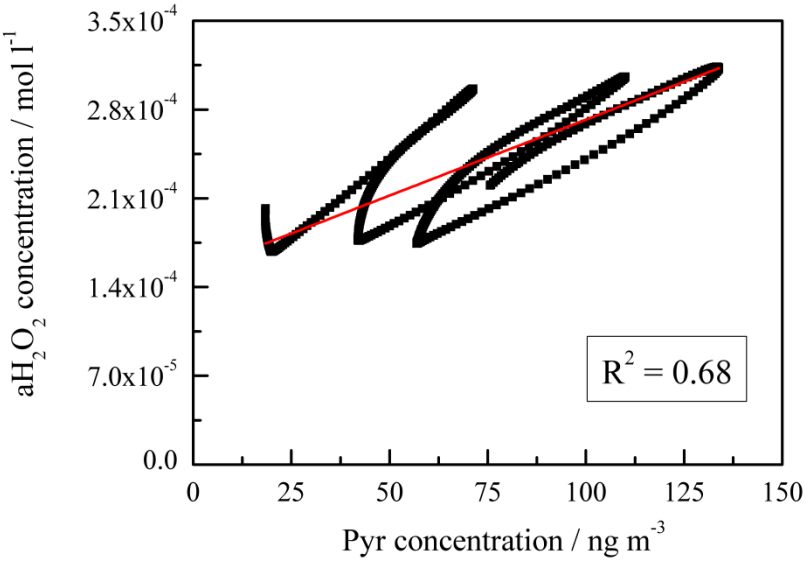

Figure S5. Scatter plot of the concentrations between Pyr and H_2O_2 in the C2wo case.

80

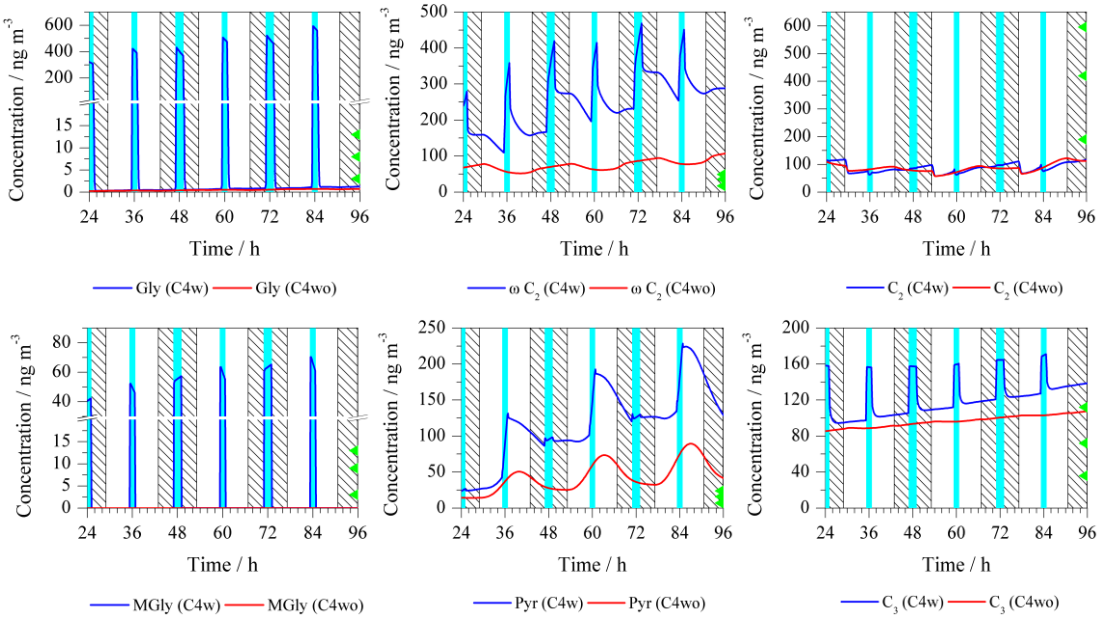

Figure S6. Time series of the modeled concentrations of selected DCRCs in the C4w and C4wo cases (light blue column: cloud; shadow: night; green triangle: maximum (above), average (middle) and minimum (below) value of measured concentration at Mt. Tai).

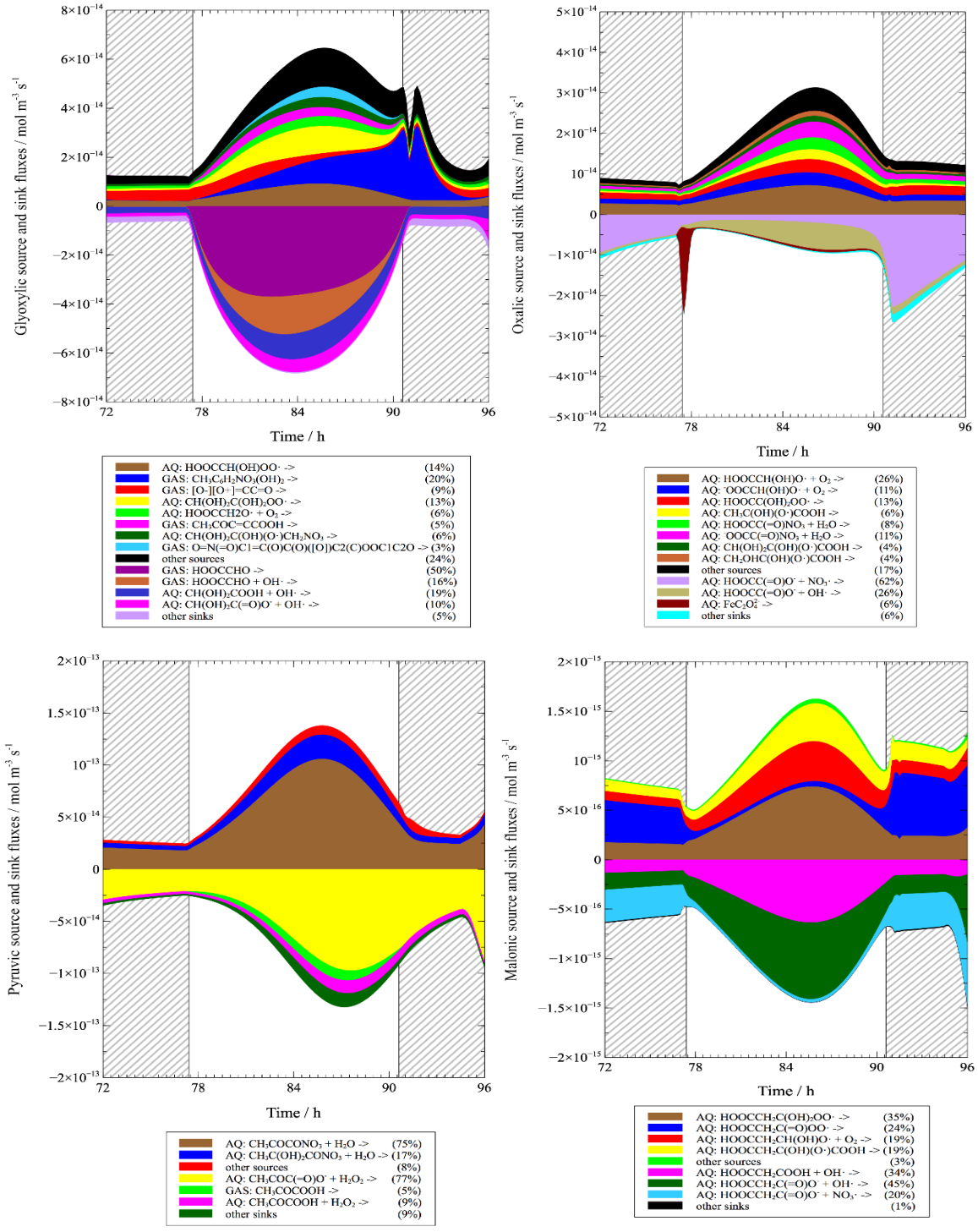

Figure S7. Modeled source and sink fluxes of glyoxylic (above left), oxalic (above right), pyruvic (below left) and malonic (below right) acid in the C2wo case (shadow: night).

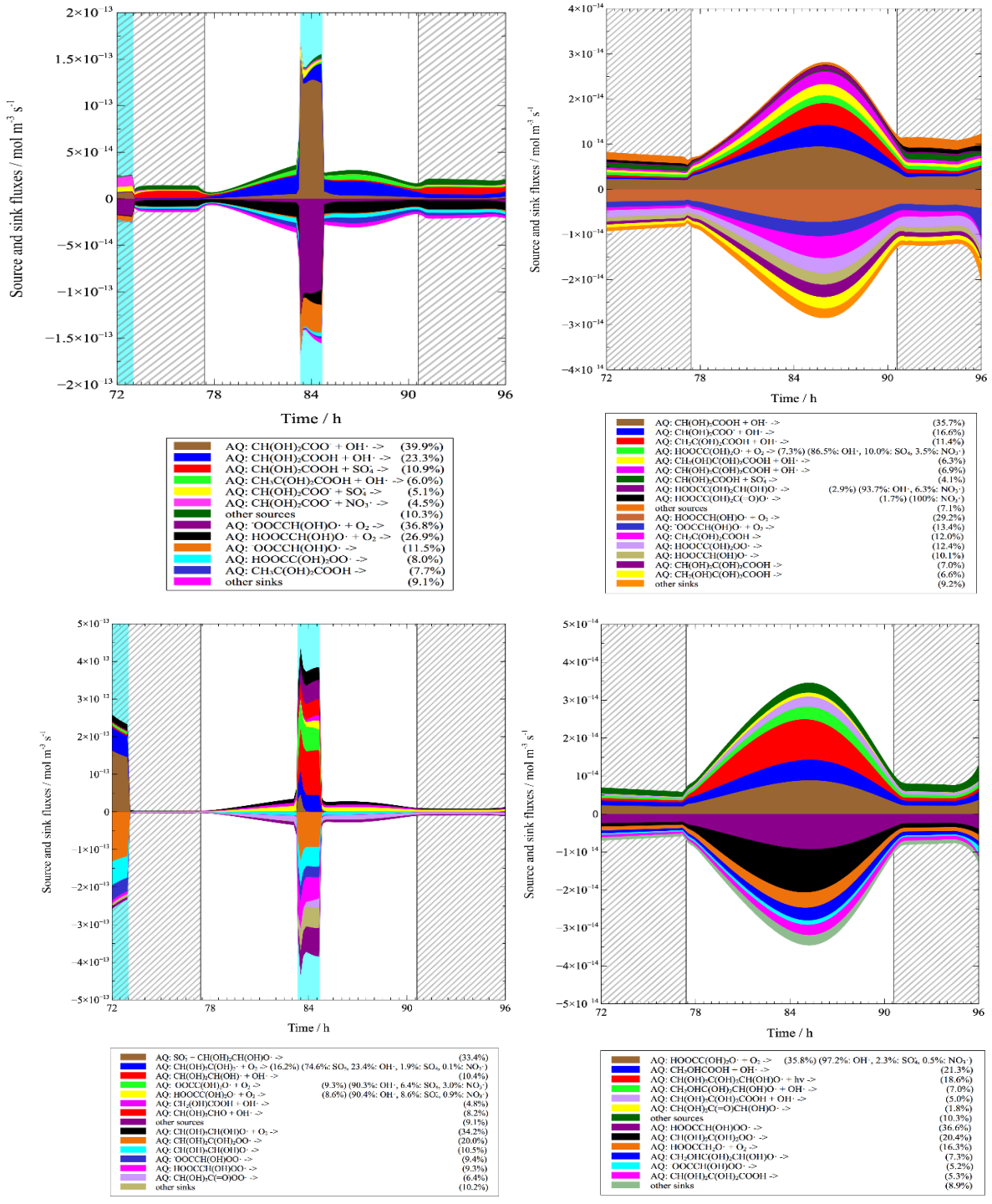

Figure S8. Key oxidants for the source compounds of oxalic (above) and glyoxylic (below) acid in the C2w (left) and C2wo (right) cases.